

## Cooling of a hot electron-hole plasma in $\text{Al}_x\text{Ga}_{1-x}\text{As}$

W. W. Rühle, K. Leo,\* and E. Bauser

*Max-Planck-Institut für Festkörperforschung, Heisenbergstrasse 1, D-7000 Stuttgart 80, Federal Republic of Germany*

(Received 8 March 1989)

Time-resolved photoluminescence experiments in the picosecond regime reveal the density dependence of the cooling of a photogenerated electron-hole plasma in  $\text{Al}_x\text{Ga}_{1-x}\text{As}$  with  $x=0-0.44$ . A strong reduction of the cooling process is observed for samples with a separation between  $\Gamma$  and  $X$  valleys larger than the LO-phonon energy. This reduction is nearly independent of the initial excess energy of the carriers. No reduction, however, is observed for samples with a direct band gap if this separation is smaller than the LO-phonon energy and for samples with indirect band gap. These results show that screening is negligible up to densities of  $7 \times 10^{17} \text{ cm}^{-3}$ . Nonthermal optical phonons created during the cooling process by intravalley scattering of electrons with small effective masses can explain the observed reduction for the electron system.

### I. INTRODUCTION

The cooling of an electron-hole plasma (EHP) in various structures of two- and three-dimensional group-III-V compounds delivers basic information about the electron-phonon interaction.<sup>1-14</sup> A reduction of the energy-loss rate by polar-optical scattering ( $\mathcal{E}_{\text{po}}$ ), i.e., the emission of LO phonons, is observed at high excitation or  $n$ -doping densities<sup>10</sup> as well in time-resolved photoluminescence (PL) experiments as in cw PL with or without electrical heating of the electron gas.<sup>1,2</sup> Two different reasons were discussed for this reduction in bulk material: (i) screening of the Fröhlich interaction at higher carrier densities,<sup>13-15</sup> or (ii) the buildup of a nonthermal phonon population<sup>4,10,16-18</sup> where the reabsorption of the LO phonons, which have a lifetime of 9 ps,<sup>19</sup> leads to a reduction of the net energy-emission rate of the carriers.

The effect which is important at the lower densities probably will also dominate the cooling behavior at higher densities. Let us make the following qualitative considerations to make this plausible: If screening would dominate at the lower densities (e.g.,  $5 \times 10^{16} \text{ cm}^{-3}$ ) it would strongly hinder the buildup of a nonthermal phonon population even at higher densities (e.g., at  $5 \times 10^{17} \text{ cm}^{-3}$ ) since the emission rate of phonons is then so strongly reduced that the phonon population remains low at all densities. In contrast, if the nonthermal phonon effect becomes important at the lower densities, the effect of screening on the  $\mathcal{E}_{\text{po}}$  will remain small even at the higher densities since screening affects both emission and reabsorption of the nonthermal phonons in about the same way. Thus, essentially, screening cannot alter the reduction of the  $\mathcal{E}_{\text{po}}$  once a nonthermal phonon population has been built up.

Previous theoretical work predicted that screening of the electron-phonon interaction should start at densities as low as  $5 \times 10^{16} \text{ cm}^{-3}$ ,<sup>15</sup> whereas according to more recent work<sup>17,18</sup> dynamical screening should set in at densities higher than  $7 \times 10^{17} \text{ cm}^{-3}$ . Experimentally, the reduction of the  $\mathcal{E}_{\text{po}}$  starts already at about  $2 \times 10^{16} \text{ cm}^{-3}$ , and a reduction by a factor of 100 is observed at

$1 \times 10^{18} \text{ cm}^{-3}$ .<sup>20</sup>

Most groups nowadays attribute this reduction to the occurrence of nonthermal phonons; however, only one experiment<sup>20</sup> has shown that screening should play a minor role up to densities of about  $4 \times 10^{17} \text{ cm}^{-3}$  by studying the reverse process, the heating of a cold EHP by a warm lattice. However, a detailed analysis reveals that the situation even in this experiment is not as simple as thought initially.<sup>21</sup> Phonon underpopulation and different temperatures of electrons and holes have both (partially compensating) influence on the heating behavior, and the absolute densities were a factor of 2 smaller than quoted in Ref. 20, as revealed by a fit of the luminescence line shape.

Thus the situation concerning screening is still not as clear as thought previously. In this paper we clarify the role of screening and additionally the question whether plasmons influence the  $\mathcal{E}_{\text{po}}$ . Finally, the role of the very initially emitted phonons is investigated. We report on two experiments: (i) the excitation photon energy  $h\nu_{\text{exc}}$  for bulk GaAs is varied between 1.55 and 1.97 eV, and (ii) we studied not only GaAs, but also  $\text{Al}_x\text{Ga}_{1-x}\text{As}$  with  $x=0-0.44$ . Particular attention was paid to samples close to the crossover composition of the ternary alloy from a semiconductor with a direct fundamental band gap to one with an indirect fundamental band gap. Three main results become evident: First, the phonons emitted in the very first relaxation process do not influence the  $\mathcal{E}_{\text{po}}$  at delay times larger than 15 ps. The  $\mathcal{E}_{\text{po}}$  is then constantly reduced and the situation actually resembles a quasi-steady-state equilibrium. Second, screening of the  $\mathcal{E}_{\text{po}}$  is a minor effect at densities up to  $n=p=7 \times 10^{17} \text{ cm}^{-3}$ , and, third, only electrons with small effective masses contribute to the reduction of the  $\mathcal{E}_{\text{po}}$  via the buildup of a strong nonthermal phonon population in a relatively small region in  $k$  space.

### II. EXPERIMENT

All samples are grown by liquid-phase epitaxy on (100)-oriented substrates. An  $\text{Al}_{0.4}\text{Ga}_{0.6}\text{As}/\text{GaAs}/\text{Al}_{0.4}\text{Ga}_{0.6}\text{As}$  heterostructure ( $d_{\text{GaAs}} \sim 0.2 \mu\text{m}$ ) is used for

TABLE I. Compilation of the sample data and results (see text). The band gap  $E_g^\Gamma$  is determined from an extrapolation of the low-energy edge of the band-to-band recombination at low excitation densities ( $\sim 10^{16} \text{ cm}^{-3}$ ). The AlAs mole fraction is calculated according to  $E_g^\Gamma = 1.519 + 1.27x \text{ eV}$ , a gauge which is obtained by a determination of  $x$  of sample 10 by a double x-ray-diffraction experiment. This gauge coincides well with the gauge given in Ref. 22. The separation between  $\Gamma$  and  $X$ ,  $\Delta E$ , is taken from Ref. 22. The last rows are the numerical results obtained as described in the text.

Sample	1	2	3	4	5	6	7	8	9	10	11
$E_g^\Gamma$ (eV)	1.519	1.677	1.755	1.806	1.895	1.982	2.003	2.032	2.038	2.043	2.080
$x$	0	0.12	0.19	0.23	0.30	0.36	0.38	0.40	0.41	0.412	0.44
$\Delta E$ (eV)	0.493	0.350	0.280	0.233	0.153	0.074	0.055	0.029	0.024	0.019	-0.014
$\alpha$ ( $n_{\text{exc}} = 7 \times 10^{17} \text{ cm}^{-3}$ )	60	50		45		40	35	25	1.5	2.5	
$\alpha$ ( $n_{\text{exc}} = 2.5 \times 10^{17} \text{ cm}^{-3}$ )	30	35	30	15	20	17	15	13	2	1.5	
$\alpha$ ( $n_{\text{exc}} = 1 \times 10^{17} \text{ cm}^{-3}$ )	15	13	10	6	8	4	3	6	1	1	
$\alpha$ ( $n_{\text{exc}} = 4 \times 10^{15} \text{ cm}^{-3}$ )		2	2	3	4	1.5	2.5	2	1	0.8	
$E_{\text{ac}}^h$ (eV)	4.8	5.6	7.3	8.0	8.6	8.8	9.1	8.6	8.2	9.4	

the experiments with variable  $h\nu_{\text{exc}}$ . Comparative experiments were carried out with GaAs single epitaxial layers ( $d = 1-2 \mu\text{m}$ ). The layers with variable AlAs mole fraction  $x$  are all single epitaxial layers ( $d = 1-2 \mu\text{m}$ ). The AlAs mole fractions of samples 10 and 11 were determined by x-ray diffraction. The data for the samples are compiled in Table I. Independent of the accuracy of the gauge of  $x$ , the decay characteristic of the PL proves that samples 1-10 are direct and that sample 11 is indirect, although the detailed situation may be rather complicated.<sup>23</sup>

The PL is excited with a synchronously pumped dye-laser [80 MHz repetition rate, 4-6 ps pulse width full width at half maximum (FWHM)]. The use of different dyes and a Lyot filter enables a tuning of the wavelength between 550 and 880 nm. The minimum size of the laser focus on the sample is  $15 \mu\text{m}$  (FWHM); however, we mostly use diameters larger than  $50 \mu\text{m}$  in order to minimize the lateral inhomogeneity of the excitation. The actual excitation densities are always determined by line-shape fits to the spectra. The luminescence light is dispersed by a 0.32-m spectrometer and is temporally resolved and detected by a two-dimensional streak camera with a typical overall time resolution of 15 ps (FWHM). The samples are always kept at about 10 K. The carrier temperature  $T_c$  at various delay times is determined from a semilogarithmic plot of the high-energy tails of the transient spectra.<sup>5,6,9,10</sup>

### III. RESULTS AND DISCUSSION

Figure 1 shows a transient spectrum of an  $\text{Al}_{0.23}\text{Ga}_{0.77}\text{As}$  single epitaxial layer 12 ps after the laser-pulse maximum, together with a theoretical line-shape fit. Rather accurate excitation densities are thus obtained. After the density is determined once, only the high-energy tails of the band-to-band recombination is traced at the different delay times.<sup>9,10</sup> The effective temperature, determined this way, mostly reflects the *electron* temperature. In this paper, however, we discuss only high-excitation effects in which electron and hole temperatures are equal<sup>12</sup> after the delay time at which we begin to ana-

lyze the data. Therefore only a common temperature  $T_c$  is used.

#### A. Results with different excitation photon energies

Figure 2 shows the cooling curve of the EHP obtained with the heterostructure and equal excitation densities, but with very different excitation photon energies  $h\nu_{\text{exc}}$ . The upper data are obtained with an excess energy  $\Delta h\nu = h\nu_{\text{exc}} - E_g^\Gamma$  of 450 meV, i.e., more than 12 times the optical-phonon energy  $\hbar\omega_{\text{LO}}$ . In the lower data,  $\Delta h\nu = 30 \text{ meV} < \hbar\omega_{\text{LO}}$ . Additional data taken with  $\Delta h\nu = 99$  and 226 meV are almost identical with the lower data set. The two lines shown are theoretical fits for  $t > 20$  ps with Fermi-Dirac statistics, screened deformation-potential scattering, and an  $\mathcal{E}_{\text{po}}$  reduced by a time-independent factor  $\alpha$  (as the only fit parameter), so that

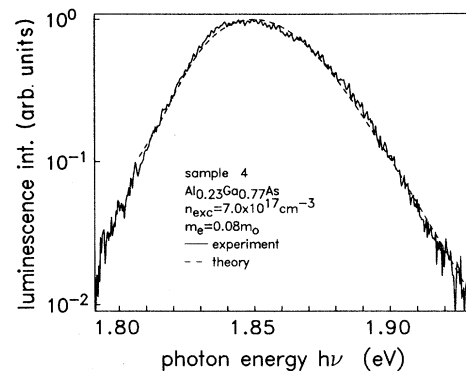


FIG. 1. Luminescence spectrum at  $t = 12$  ps of an  $\text{Al}_{0.23}\text{Ga}_{0.77}\text{As}$  sample (solid line) with a theoretical line-shape fit (dashed line). In these line-shape fits the change of the electron effective mass  $m_e$  with the AlAs mole fraction  $x$  is taken into account.

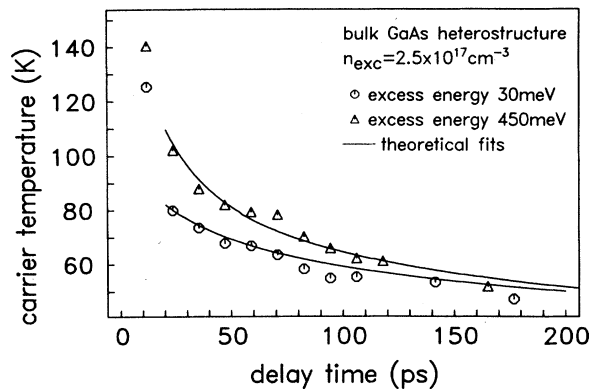


FIG. 2. Cooling curve of the EHP for different initial excess energy  $\Delta h\nu$  of the carriers. Delay time 0 is at the maximum of the laser pulse. The fit starts at 20 ps, i.e., when the laser pulse is over. The experimental temperatures at 12 ps are included to demonstrate that the fit with a constant reduction  $\alpha$  of the  $\mathcal{E}_{po}$  cannot explain the initial temperature decay.

$$\alpha = \mathcal{E}_{po}^{\text{theor}} / \mathcal{E}_{po}^{\text{expt}},$$

where  $\mathcal{E}_{po}^{\text{theor}}$  is calculated with an unscreened Fröhlich interaction and with the phonons in equilibrium with the lattice. Details of the fit procedures are given in Refs. 9–11. The material parameters, which we use, are compiled in Table II.

Figure 3 shows  $\alpha$  and the initial  $T_c^i$ , directly, i.e., 20 ps after the laser pulse for the four different  $\Delta h\nu$  at an excitation density of  $2.5 \times 10^{17} \text{ cm}^{-3}$ . Obviously,  $\alpha$  and  $T_c^i$  do not depend on  $\Delta h\nu$  if  $\Delta h\nu < 300 \text{ meV}$ . Only for the largest  $\Delta h\nu$  is  $T_c^i$  slightly higher. In this case the energy of the electrons is large enough to enable scattering into the  $L$  minima. This scattering process is fast; however, the process back lasts a few ps,<sup>24</sup> which might lead to a delayed heating effect, resulting in a larger  $T_c^i$ .

At first sight, the independence of  $\alpha$  on the number of initially emitted phonons appears as an argument favoring screening as the origin for the reduction of the  $\mathcal{E}_{po}$  at these densities. A closer look, however, reveals that the

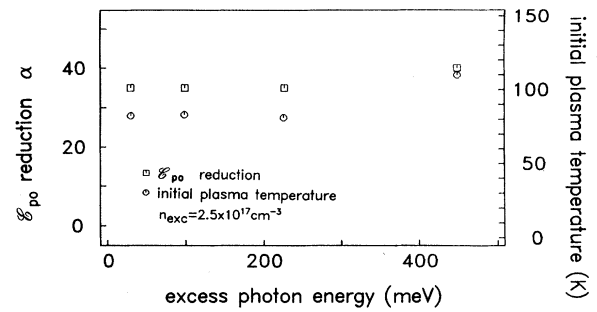


FIG. 3. Reduction of the energy-loss rate  $\alpha$  (left scale) and the initial plasma temperature  $T_c^i$ , 20 ps after the laser pulse (right scale) as a function of the initial excess energy of the carriers.

assumption of nonthermal phonons is also consistent with this result: The phonons emitted by electrons high up in the  $\Gamma$  valley have very small  $k$  values. Such phonons cannot be reabsorbed—due to  $k$  conservation—by a thermalized electron gas which is, for  $T_c \sim 100 \text{ K}$ , close to the bottom of the  $\Gamma$  valley where the electron dispersion curve is less steep. On the other hand, this result strongly supports the conception that the cooling on our time scale resembles a quasi-steady-state equilibrium, where the nonequilibrium phonon population is quasipermanently maintained by the generation and reabsorption of phonons due to the cooling of the EHP and the anharmonic decay of optical into acoustical phonons.

Figure 4 shows  $\alpha$  as a function of excitation density for both the heterostructure and a single epitaxial layer, with  $\Delta h\nu \sim 100 \text{ meV}$ . A strong increase of  $\alpha$  is observed for densities larger than  $2 \times 10^{16} \text{ cm}^{-3}$ . We note that the results for the two samples only fall together if the densities are determined from the spectra and are not calculated from the laser power, the absorption coefficient, etc. Fast vertical diffusion obviously strongly reduces the density in the case of single epitaxial layers since we get, for the same laser intensity, a factor-of-3-lower carrier density than for the heterostructure. Obviously, it is absolutely necessary to determine densities by line-shape fits and not

TABLE II. Material parameters used in the fits and calculations.

Electron effective mass <sup>a</sup>	$(0.067 + 0.083x)m_0$
Hole effective mass <sup>a</sup>	$(0.50 + 0.14x)m_0$
Static dielectric constant <sup>b</sup>	12.75
Optical dielectric constant <sup>b</sup>	10.94
LO-phonon energy <sup>b</sup>	36.4 meV
Electron deformation potential <sup>c</sup>	7.0 eV
Hole deformation potential $E_{ac}^h$ (see text)	4.8–9 eV
Density of GaAs <sup>a</sup>	$5.32 - 1.6x \text{ g cm}^{-3}$

<sup>a</sup>From S. Adachi, J. Appl. Phys. **58**, R1 (1985).

<sup>b</sup>Semiconductors, Vol. 17 of *Landolt-Börnstein*, New Series, edited by K. H. Hellwege (Springer, Berlin, 1982).

<sup>c</sup>From D. L. Rode, Phys. Rev. **B 2**, 1012 (1970).

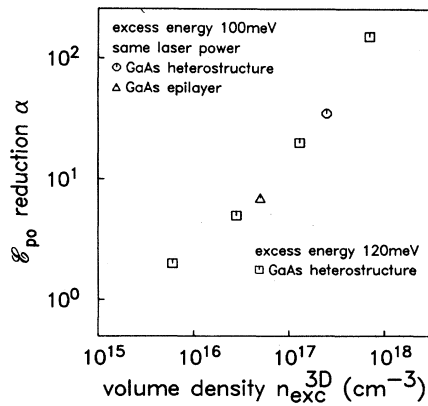


FIG. 4. Reduction of the energy-loss rate of the EHP as a function of carrier density determined by a line-shape fit.

from the experimental conditions.

We have calculated a qualitative model of the hot phonon reabsorption for the two-dimensional (2D) case<sup>10</sup> and a quantitative model for the three-dimensional (3D) case.<sup>25</sup> Both nicely explain why the reduction  $\alpha$  is independent of  $T_c$  and therefore independent of time on a time scale of about 100 ps, i.e., a time much longer than the LO-phonon lifetime. A quantitative agreement, however, is obtained for electrons only. The hole-phonon interaction dissipates energy faster than we would expect from our experiments: The detailed model,<sup>25</sup> which takes into account electron-hole, electron-LO-phonon, and hole-LO- and -TO-phonon interactions, delivers  $\alpha=7$  for  $n_{exc}=1 \times 10^{18} \text{ cm}^{-3}$ , whereas the experiment reveals  $\alpha=100$ . The good agreement between theory<sup>16</sup> and former experimental results appears accidentally: a re-evaluation of the old spectra reveals<sup>25</sup> that the density was more than an order of magnitude lower in these experiments than quoted in Ref. 14. The detailed model<sup>25</sup> explains why we get at the lowest densities  $\alpha=2$  and not  $\alpha=1$ , i.e., exactly the theoretical  $\mathcal{E}_{po}$ : nonequilibrium occurs between electron and holes—the holes are always

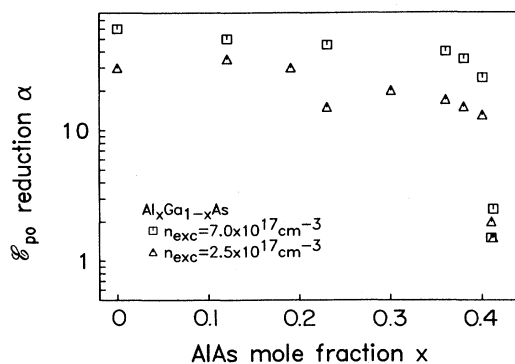


FIG. 5. Reduction  $\alpha$  of the energy-loss rate as a function of the AlAs mole fraction  $x$  for two different, high-excitation densities  $n_{exc}$ .

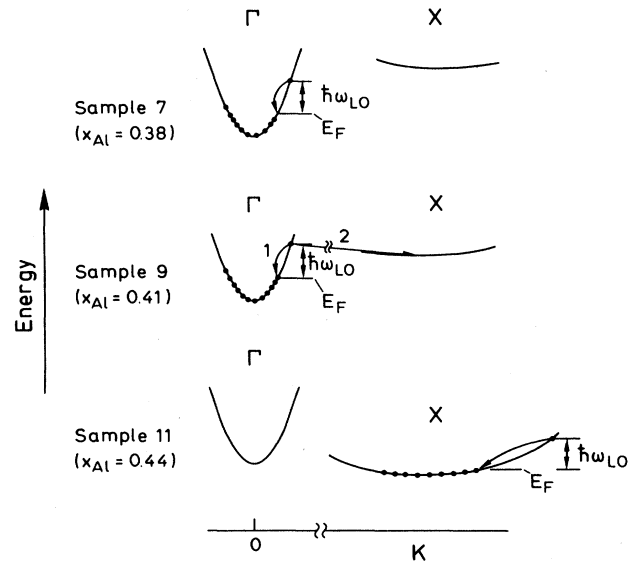


FIG. 6. Sketch of the different possible scattering processes for samples with an AlAs mole fraction close to the crossover composition, where  $\text{Al}_x\text{Ga}_{1-x}\text{As}$  becomes an indirect-gap semiconductor.

colder than the electrons at the lower densities, so essentially the electrons contribute to the cooling only, but both carriers contribute to the specific heat.

## B. Results on $\text{Al}_x\text{Ga}_{1-x}\text{As}$

Next, we consider the results with  $\text{Al}_x\text{Ga}_{1-x}\text{As}$ . In these experiments we always choose  $\hbar\nu_{exc}=E_g+100 \text{ meV}$ . Figure 5 shows  $\alpha$  as a function of  $x$  for all direct-gap samples. In the theoretical fits we still assume that only the GaAs-like modes contribute to the energy loss in the interesting temperature range due to their smaller energy. The reduction  $\alpha$  decreases only slowly for increas-

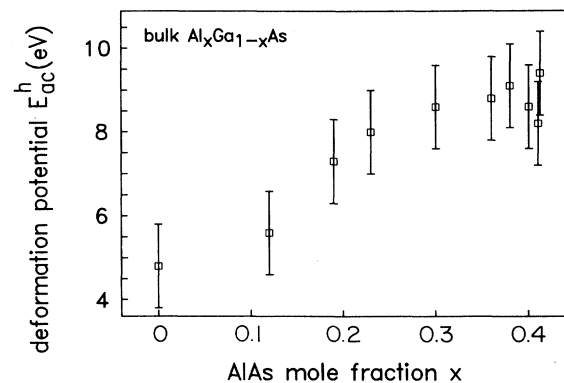


FIG. 7. Dependence of the deformation potential of the holes  $E_{ac}^h$  on the AlAs mole fraction  $x$  if the variation of scattering at low temperatures with  $x$  is attributed to a change in deformation potential.

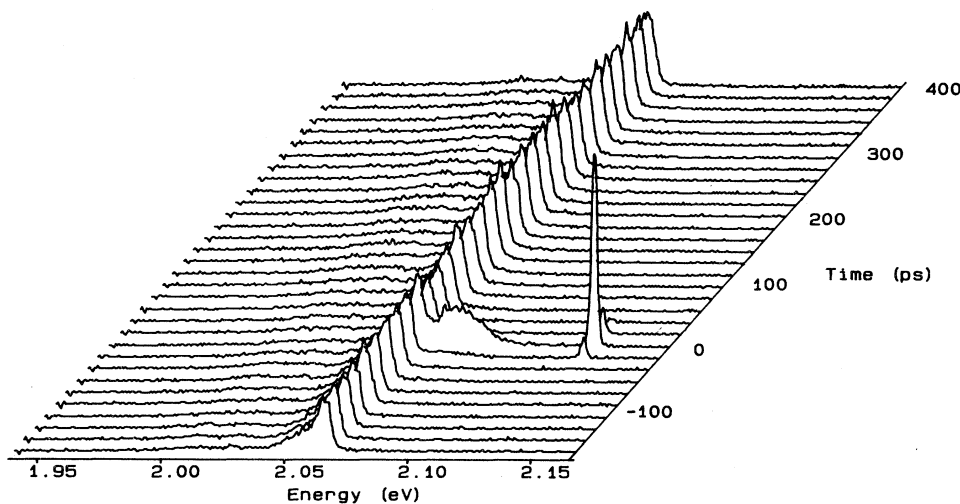


FIG. 8. Three-dimensional plot of the time behavior of the photoluminescence of the indirect  $\text{Al}_{0.44}\text{Ga}_{0.56}\text{As}$  sample. The luminescence at about 2.06 eV originates from electrons in the  $X$  valleys and has a decay time longer than the repetition time of the laser pulses. Scattered light of the laser pulse appears at 2.16 eV, and the fast luminescence flash at 2.08 eV originates from electrons in the  $\Gamma$  valley.

ing  $x$  as long as  $x < 0.4$ , an effect which might be explained by the increase of the effective masses with  $x$  (not taken into account in the  $\epsilon_{\text{po}}$ ). However, a clear jump is observed at  $x \sim 0.4$ : for  $x > 0.4$  the  $\epsilon_{\text{po}}$  is close to theory;  $\alpha$  becomes independent of excitation density, and is always close to 2. We note that the fast PL decay clearly reveals that samples 9 and 10 still have a direct fundamental energy gap. A sketch of the energetic position of the different minima of the most interesting samples is shown in Fig. 6. The separation between the Fermi level in the  $\Gamma$  minimum and the bottom of the  $X$  minima is, for samples 1–8, larger than the energy of the LO phonon at  $\Gamma$  or  $X$ , i.e., phonon emission into the “bottleneck” on the LO branch can only occur via intraband scattering in the  $\Gamma$  valley. As a consequence, we get the same nonthermal phonon effects as in GaAs. Samples 9 and 10 are still direct and most of the carriers are still in the  $\Gamma$  valley. However, electrons with an excess energy of  $\hbar\omega_{\text{LO}}(X)$  now have the possibility to undergo an intervalley deformation potential scattering process with a zone-boundary LO phonon, which has a much larger  $k$  vector. No appreciable nonthermal phonon population can be generated by such a process since the volume in  $k$  space in which the phonons are created is very large.

On the other hand, screening in an EHP is determined by the particles with the larger Debye vectors—the holes. From samples 7 and 8 to samples 9 and 10, only the scattering possibilities of the electrons, and neither the screening of electrons nor holes, is changed. Therefore this experiment shows that the reduction of the  $\epsilon_{\text{po}}$  is not caused by screening. Plasmons also cannot influence the  $\epsilon_{\text{po}}$  since they are almost identical for samples 7–10.

The deformation-potential scattering determines the energy-loss rate at lower temperatures and shows a pronounced dependence on  $x$ . Taking into account the

dependence of the hole effective mass and of the density  $\rho$  on  $x$ , we get a variation of the hole deformation potential with  $x$  shown in Fig. 7. The origin of this dependence and whether it is really a change in deformation potential is not yet clear. It is almost impossible to detect this effect in transport experiments, since alloy scattering also changes with  $x$ .

Finally, sample 11 clearly has an indirect fundamental band gap. Figure 8 shows a three-dimensional plot of the time-resolved PL. The decay time of the luminescence is of the order of the time between two laser pulses (12.5 ns); therefore luminescence from the preceding pulse is still observed at negative times before pulse arrival. During the laser pulse (at  $t = 0$ ), luminescence originating from electrons in the  $\Gamma$  valley is visible at 2.08 eV. This luminescence decays much faster than our optimum time resolution ( $1/e$  decay faster than 3 ps). A minimum lifetime of the carriers in the  $\Gamma$  valley of 35 fs can be estimated from the linewidth of this luminescence flash if a homogeneous broadening of the line is assumed.

Cooling by polar-optical scattering is, in the case of this indirect semiconductor, extremely fast. The temperature of the EHP falls within our time-resolution immediately below 40 K, i.e., into a temperature range where LO-phonon emission is negligible against the emission of acoustical phonons.

#### IV. CONCLUSIONS

We have shown that screening and other plasmon effects do not influence the polar-optical energy-loss rate up to EHP densities of  $7 \times 10^{17} \text{ cm}^{-3}$ . The much smaller  $\epsilon_{\text{po}}$  observed at these densities is most likely caused by the reabsorption of nonthermal phonons generated by electrons with a small effective mass in a small volume in  $k$  space. Nonthermal phonon effects are much smaller

for holes and for electrons in  $X$  valleys due to their larger effective masses. In particular, we expect these effects not to be important, e.g., in Si. The detailed role of the energy dissipation by the holes is not yet clear. Possibly the degeneracy of the valence band<sup>26</sup> and the influence of many-particle effects on the high-energy tail of the photoluminescence<sup>27</sup> cause effects not considered in this publication.

In time-resolved experiments in the picosecond regime the initially emitted phonons do not contribute to the nonthermal phonon effect at times  $> 20$  ps. The situation rather resembles a quasi-steady-state equilibrium, in which a high-density thermalized electron gas generates and maintains its nonthermal phonon population in such

a way that the  $\mathcal{E}_{\text{po}}$  is nearly independent of temperature always reduced by a constant amount solely determined by the carrier density.

#### ACKNOWLEDGMENTS

We would like to thank H. Kalt, J. Collet, and P. Kocevar for helpful discussions, J. Nagle for the x-ray experiments, J. Kuhl for a critical reading of the manuscript, and K. Rother and H. Klann for expert technical assistance. The financial support of the Bundesministerium für Forschung und Technologie is gratefully acknowledged.

\*Present address: AT&T Bell Laboratories, Holmdel, NJ 07733.

<sup>1</sup>J. Shah, IEEE J. Quantum Electron. (to be published).

<sup>2</sup>S. Lyon, J. Lumin. **35**, 121 (1986).

<sup>3</sup>K. Kash, J. Shah, D. Block, A. C. Gossard, and W. Wiegmann, Physica B+C **134B**, 189 (1985).

<sup>4</sup>J. Shah, A. Pinczuk, A. C. Gossard, and W. Wiegmann, Phys. Rev. Lett. **54**, 2045 (1985).

<sup>5</sup>H. Lobentanzer, H. J. Polland, W. W. Rühle, W. Stolz, and K. Ploog, Phys. Rev. B **36**, 1136 (1987).

<sup>6</sup>H. Lobentanzer, H. J. Polland, W. W. Rühle, W. Stolz, and K. Ploog, Appl. Phys. Lett. **51**, 673 (1987).

<sup>7</sup>H. Lobentanzer, W. W. Rühle, H. J. Polland, W. Stolz, and K. Ploog, Phys. Rev. B **36**, 2954 (1987).

<sup>8</sup>H. J. Zarrabi and R. R. Alfano, Phys. Rev. B **32**, 3947 (1985).

<sup>9</sup>K. Leo, W. W. Rühle, H. J. Queisser, and K. Ploog, Phys. Rev. B **37**, 7121 (1988).

<sup>10</sup>K. Leo, W. W. Rühle, and K. Ploog, Phys. Rev. B **38**, 1947 (1988).

<sup>11</sup>K. Leo and W. W. Rühle, Solid State Commun. **62**, 659 (1987).

<sup>12</sup>J. H. Collet, K. Leo, and W. Rühle (unpublished).

<sup>13</sup>J. Shah, Solid State Electron. **21**, 43 (1978).

<sup>14</sup>W. Graudszus and E. O. Göbel, Physica B+C **117&118B**, 555 (1983).

<sup>15</sup>E. J. Yoffa, Phys. Rev. B **21**, 2415 (1980); **23**, 1909 (1981).

<sup>16</sup>P. Kocevar, Physica B+C **134B**, 155 (1985).

<sup>17</sup>S. Das Sarma, J. K. Jain, and R. Jalabert, Phys. Rev. B **37**, 6290 (1988).

<sup>18</sup>J. H. Collet Phys. Rev. B **39**, 7659 (1989).

<sup>19</sup>J. A. Kash and J. C. Tsang, Solid State Electron. **31**, 419 (1988).

<sup>20</sup>W. W. Rühle and H. J. Polland, Phys. Rev. B **36**, 1683 (1987).

<sup>21</sup>K. Leo, W. W. Rühle, and K. Ploog (unpublished).

<sup>22</sup>D. J. Wolford, W. Y. Hsu, J. D. Dow, and B. G. Streetman, J. Lumin. **18/19**, 863 (1978).

<sup>23</sup>H. Kalt and W. W. Rühle (unpublished).

<sup>24</sup>J. Shah, B. Deveaud, T. C. Damen, W. T. Tsang, A. C. Gossard, and P. Lugli, Phys. Rev. Lett. **59**, 2222 (1987).

<sup>25</sup>K. Leo, Ph.D. thesis, University of Stuttgart, 1988.

<sup>26</sup>R. P. Joshi and D. K. Ferry, Phys. Rev. B **36**, 1180 (1989).

<sup>27</sup>J. H. Collet, W. W. Rühle, M. Pugno, K. Leo, and A. Million (unpublished).